Enzyme Models

DOI: 10.1002/anie.201404556

Demonstration of the Heterolytic O–O Bond Cleavage of Putative Nonheme Iron(II)–OOH(R) Complexes for Fenton and Enzymatic Reactions**

*Suhee Bang, Sora Park, Yong-Min Lee, Seungwoo Hong, Kyung-Bin Cho, and Wonwoo Nam**

Abstract: *One-electron reduction of mononuclear nonheme iron(III) hydroperoxo (Fe^{III}–OOH) and iron(III) alkylperoxo (Fe^{III}–OOR) complexes by ferrocene (Fc) derivatives resulted in the formation of the corresponding iron(IV) oxo complexes. The conversion rates were dependent on the concentration and oxidation potentials of the electron donors, thus indicating that the reduction of the iron(III) (hydro/alkyl)peroxo complexes to their one-electron reduced iron(II) (hydro/alkyl)peroxo species is the rate-determining step, followed by the heterolytic O–O bond cleavage of the putative iron(II) (hydro/alkyl)peroxo species to give the iron(IV) oxo complexes. Product analysis supported the heterolytic O–O bond-cleavage mechanism. The present results provide the first example showing the one-electron reduction of iron(III) (hydro/alkyl)peroxo complexes and the heterolytic O–O bond cleavage of iron(II) (hydro/alkyl)peroxo species to form iron(IV) oxo intermediates which occur in nonheme iron enzymatic and Fenton reactions.*

Mononuclear nonheme iron complexes coordinating hydroperoxo and alkylperoxo ligands, such as Fe^{n+}–OOH and Fe^{n+}–OOR, are key intermediates in the catalytic activation of dioxygen by nonheme iron enzymes and bleomycins.[1] The peroxide ligands of the iron hydroperoxo and alkylperoxo species are cleaved either homolytically or heterolytically to form high-valent iron oxo intermediates. In biomimetic studies, a large number of mononuclear nonheme iron(III) hydroperoxo (Fe^{III}–OOH) and iron(III) alkylperoxo (Fe^{III}–OOR) complexes have been synthesized and used in the investigation of the chemical and physical properties of the peroxide ligands, along with the mechanism of the peroxide O–O bond cleavage.[2,3] Very recently, it has been shown that the peroxide ligands of high-spin iron(III) (hydro/alkyl)peroxo complexes bearing macrocyclic *N*-tetramethylated cyclam (TMC) ligands are cleaved homolytically, thus resulting in the formation of iron(IV) oxo complexes (Scheme 1 a, pathway A).[4]

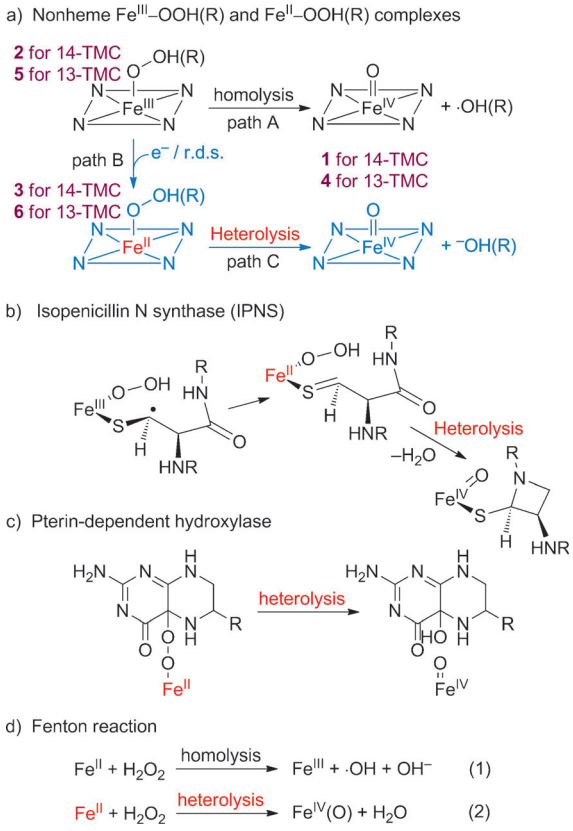

Scheme 1. Proposed mechanisms for the homolytic and heterolytic O–O bond cleavage of Fe^{n+}–OOH(R) species.

Iron(II) (hydro/alkyl)peroxo complexes, which are one-electron-reduced species of iron(III) (hydro/alkyl)peroxo complexes, have also been proposed as intermediates in nonheme iron enzymes, such as isopenicillin N synthase (IPNS) and pterin-dependent hydroxylases.[5,6] In IPNS, an iron(II) hydroperoxo species, which is formed by one-electron transfer to an iron(III) hydroperxo species, is converted into an iron(IV) oxo intermediate by O–O bond heterolysis (Scheme 1 b).[5] In pterin-dependent hydroxylases, iron(II) alkylperoxo intermediates are converted into iron(IV) oxo species by heterolytic O–O bond cleavage (Scheme 1 c).[6] However, evidence for the conversion of the iron(II) (hydro/alkyl)peroxo species into the corresponding iron(IV) oxo species by heterolytic O–O bond cleavage has yet to be obtained in nonheme iron enzymatic and biomimetic reactions.

In Fenton chemistry, the nature of the active oxidant and the mechanism of the O–O bond cleavage in the reaction of

[*] S. Bang, S. Park, Dr. Y.-M. Lee, Dr. S. Hong, Dr. K.-B. Cho, Prof. Dr. W. Nam
Department of Chemistry and Nano Science
Ewha Womans University, Seoul 120–750 (Korea)
E-mail: wwnam@ewha.ac.kr

[**] We gratefully acknowledge research support of this work from the NRF of Korea through CRI (NRF-2012R1A3A2048842 to W.N.) and GRL (NRF-2010-00353 to W.N.) and Basic Science Research Program (2013R1A1A2062737 to K.-B.C.).

Supporting information for this article is available on the WWW under http://dx.doi.org/10.1002/anie.201404556.

 © 2014 Wiley-VCH Verlag GmbH & Co. KGaA, Weinheim

an iron(II) salt and H_2O_2 has attracted much attention for more than 100 years.[7] As shown in Scheme 1 d, a homolytic O–O bond cleavage of H_2O_2 affords a free ·OH radical [Eq. (1)], whereas an iron(IV) oxo is formed by heterolytic O–O bond cleavage of a putative Fe^{II}–H_2O_2 species [Eq. (2)]. Very recently, Que and co-workers reported a clean formation of an iron(IV) oxo complex, $[(14\text{-TMC})Fe^{IV}(O)]^{2+}$ (**1**; 14-TMC = 1,4,8,11-tetramethyl-1,4,8,11-tetraazacyclotetradecane), in the reaction of $[Fe^{II}(14\text{-TMC})]^{2+}$ and a stoichiometric amount of H_2O_2 in the presence of a base (e.g., 2,6-lutidine).[8a] Density functional theory (DFT) calculations proposed that **1** was formed by a combination of partial homolytic O–O bond cleavage and proton-coupled electron transfer (PCET) of an iron(II)/H_2O_2 species.[8b] However, the mechanism was proposed based on indirect experimental evidence without detecting any intermediates (e.g., Fe^{II}/H_2O_2). In the case of nonheme Fe^{II}–OOR species (e.g., proposed intermediates of pterin-dependent hydroxylases), no detailed mechanistic studies have been conducted so far for the alkylperoxo O–O bond cleavage steps.

Herein we report that one-electron reduction of iron(III) (hydro/alkyl)peroxo complexes by ferrocene (Fc) derivatives resulted in the formation of their corresponding iron(IV) oxo complexes. Based on detailed mechanistic studies, we have proposed that the one-electron reduction of the iron(III) (hydro/alkyl)peroxo complexes by Fc derivatives is the rate determining step (Scheme 1 a, pathway B) and that the resulting iron(II) (hydro/alkyl)peroxo intermediates are converted into iron(IV) oxo complexes by heterolytic O–O bond cleavage (Scheme 1 a, pathway C).

The iron(III) hydroperoxo complex, $[(14\text{-TMC})Fe^{III}\text{-OOH}]^{2+}$ (**2**), was prepared by adding 3 equivalents of $HClO_4$ to a solution of $[(14\text{-TMC})Fe^{III}(O_2)]^{+}$ in acetone/CF_3CH_2OH (v/v 3:1) at −40 °C under an argon atmosphere, as reported previously.[4a] Interestingly, addition of one equivalent of Fc to the solution of **2** resulted in the disappearance of the absorption peak at $\lambda = 526$ nm, which corresponds to **2**, with the concomitant appearance of absorption peaks at $\lambda =$ 810 nm corresponding to **1** and at $\lambda = 620$ nm corresponding to ferrocenium cation (Fc^+).[9] The reaction was complete within 2 seconds and a clear isosbestic point at $\lambda = 727$ nm was observed in the titration experiment (Figure 1 a, and see Figure S1 in the Supporting Information). The titration experiment revealed that one equivalent of Fc was required for the full conversion of **2** into **1** (Figure 1 a, inset). We then examined the concentration effect of Fc on the rate of the conversion of **2** into **1**. The conversion rate increased linearly with the increase of the Fc concentration under pseudo-first-order reaction conditions (e.g., with > 10 equiv of Fc), and a second-order rate constant, k_2, was determined to be $8.1(6) \times 10^3\ M^{-1}s^{-1}$ at −40 °C (see Figure S2 a). We also found that the rates of the electron transfer from Fc derivatives to **2** were dependent on the oxidation potentials of the Fc derivatives. As observed in the case of Fc, the electron-transfer rates from Fc derivatives to **2** increased with the increase of the concentration of Fc derivatives (Figure S2), and the conversion of **2** into **1** was faster with electron donors having lower oxidation potential (see Figure 1 b and Table S1). Based on the observations that the rate of the conversion of **2** into **1** was dependent on the concentration of electron donors and that the rates were different depending on the electron donors, we propose that one-electron reduction of **2** by the electron donors (e.g., Fc derivatives) to afford a one-electron reduced species, $[(14\text{-TMC})Fe^{II}\text{-OOH}]^{+}$ (**3**), is the rate-determining step (Scheme 1 a, pathway B), with subsequent fast conversion of **3** into **1** by O–O bond cleavage (Scheme 1 a, pathway C). It should be noted that the negative slope of −9.7(6) in Figure 1 b for **2** is slightly larger than that obtained from outer-sphere electron-transfer reduction of **1** (slope = −8.2)[10] at 25 °C, but slightly smaller than that of Fe^{III}–$OOSc^{3+}$ (slope = −12)[11a] at −40 °C, thus suggesting that the rate dependence on the oxidation potential of the reductant follows the Marcus theory of electron transfer.

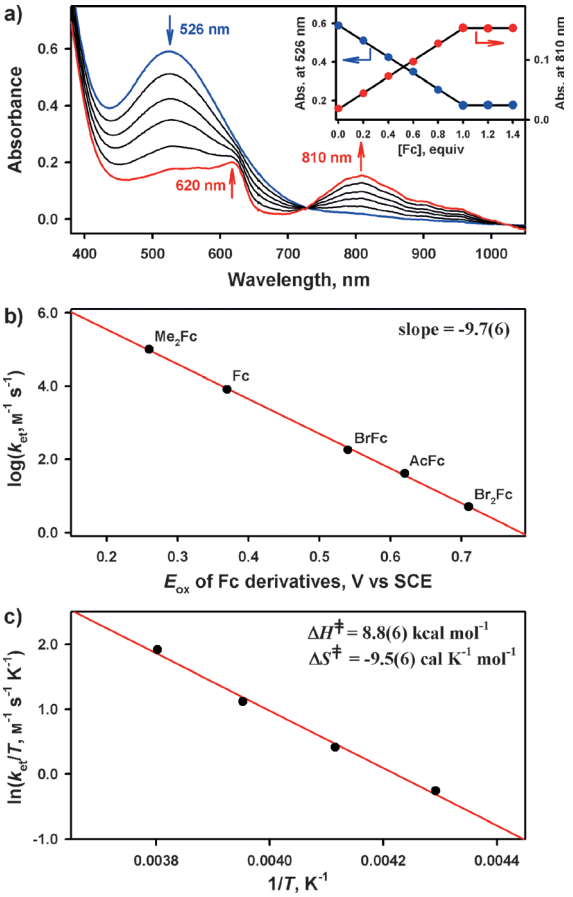

Figure 1. a) UV/Vis spectral changes showing the disappearance of the peak for $[(14\text{-TMC})Fe^{III}\text{-OOH}]^{2+}$ (**2**) at $\lambda = 526$ nm with the concomitant appearance of the peaks for $[(14\text{-TMC})Fe^{IV}(O)]^{2+}$ (**1**) at $\lambda = 810$ nm and Fc^+ at $\lambda = 620$ nm by addition of Fc (0–1.0 equiv) to a solution of **2** (0.50 mM, blue line) in increments of 0.20 equiv in acetone/CF_3CH_2OH (v/v 3:1) at −40 °C. Inset shows the spectroscopic titration at $\lambda = 526$ nm for the disappearance of **2** (blue circles) and $\lambda = 810$ nm for the formation of **1** (red circles) as a function of the number of equivalents of Fc (0–1.4 equiv) added to the solution of **2** in increments of 0.20 equiv. b) Plot of ln k_{et} against the E_{ox} of electron donors obtained in the electron-transfer reaction from Fc derivatives to **2** in acetone/CF_3CH_2OH (v/v 3:1) at −40 °C. c) The Eyring plot for electron transfer from bromoferrocene (BrFc) to **2** in acetone/CF_3CH_2OH (v/v 3:1) at 233–263 K.

© 2014 Wiley-VCH Verlag GmbH & Co. KGaA, Weinheim

We also investigated the reaction of an iron(III) alkylhydroperoxo complex, $[(13\text{-TMC})Fe^{III}\text{-}OOC(CH_3)_3]^{2+}$ (**5**; 13-TMC = 1,4,7,10-tetramethyl-1,4,7,10-tetraazacyclotridecane; see Figure S3a),[4d] with Fc derivatives in acetone/CF_3CH_2OH (v/v 3:1) at −40 °C. Addition of one equivalent of Fc to the solution of **5** resulted in the disappearance of the absorption peak at $\lambda = 520$ nm, which corresponds to **5**, with the concomitant appearance of absorption peaks at $\lambda = 740$ nm, corresponding to $[(13\text{-TMC})Fe^{IV}(O)]^{2+}$ (**4**),[4d,12] and at $\lambda =$ 620 nm, corresponding to Fc^+ (Figure 2a).[9] The reaction was complete within 1 second (see Figure S4). When the concentration effect of Fc on the rate of the conversion of **5** into **4** was investigated under pseudo-first-order reaction conditions (e.g., with > 10 equiv of Fc), the rate of the electron transfer from Fc to **5** increased linearly with the increase of the Fc concentration, and a second-order rate constant, k_2, was determined to be $3.5(4)\times10^3\,M^{-1}s^{-1}$ at −40 °C (see Figure S5a). This reaction is slightly slower than that of **2** and Fc (e.g., $8.1(6)\times10^3\,M^{-1}s^{-1}$). As we have observed in the reactions of **2** and Fc derivatives, the electron-transfer rates from Fc derivatives to **5** were dependent on the oxidation potentials of the Fc derivatives (Table S1 and Figure S5). The conversion of **4** into **5** was faster with electron donors having lower oxidation potential (Figure 2b). Based on the observations that the rate of the conversion of **5** into **4** was dependent on the concentration of electron donors and that the rates were different depending on the electron donors, we propose that the reduction of **5** by the electron donors (e.g., Fc derivatives) to give a one-electron reduced species, $[(13\text{-TMC})Fe^{II}\text{-}OOC(CH_3)_3]^+$ (**6**) is the rate-determing step (Scheme 1a, pathway B), with subsequent fast conversion of **6** into **4** by O–O bond cleavage (Scheme 1a, pathway C). The slope of −12(1) in Figure 2b for **5** is quite similar to that reported for outer-sphere electron-transfer reduction of Fe^{III}–$OOSc^{3+}$ (−12)[11a] at −40 °C, thus suggesting that the rate dependence on the oxidation potential of the reductant follows the Marcus theory of electron transfer.

We also determined the activation parameters of electron transfer from bromoferrocene (BrFc) to iron(III) (hydro/alkyl)peroxo complexes, such as $[(14\text{-TMC})Fe^{III}\text{-}OOH]^{2+}$ (**2**) and $[(13\text{-TMC})Fe^{III}\text{-}OOC(CH_3)_3]^{2+}$ (**5**), by determining the reaction rates at different temperatures (Figures 1c and 2c for the reactions of **2** and **5**, respectively; see also Table S2 and Figure S6). The small, negative $\Delta S^{\ddagger}$ values indicate that the electron transfer from Fc derivatives to the iron(III) (hydro/alkyl)peroxo complexes occurs through outer-sphere electron-transfer reactions, as reported in the electron-transfer reactions of metal–oxygen intermediates.[13]

Then, how are the O–O bonds of the hydroperoxo and alkylperoxo ligands of **2** and **5** cleaved to form their corresponding iron(IV) oxo species, such as **1** and **4**, respectively? Since cumyl hydroperoxide (CmOOH) is a well-known mechanistic probe which can be used to distinguish homolytic versus heterolytic O–O bond cleaving pathways,[4d,14] the product(s) formed in the reaction of $[(13\text{-TMC})Fe^{III}\text{-}OOCm]^{2+}$ (Figure S3b) with one equivalent of Fc was analyzed. The product analysis revealed the exclusive formation of cumyl alcohol (ca. 90%) with no formation of acetophenone (see the Experimental Section in the Supporting Information). The observation of the cumyl alcohol formation as a sole product in the reaction of **5** and Fc demonstrates unambiguously that the conversion of **6**, which is the product of one-electron reduction of **5** by Fc, into **4** occurs exclusively by an O–O bond heterolysis (Scheme 2).

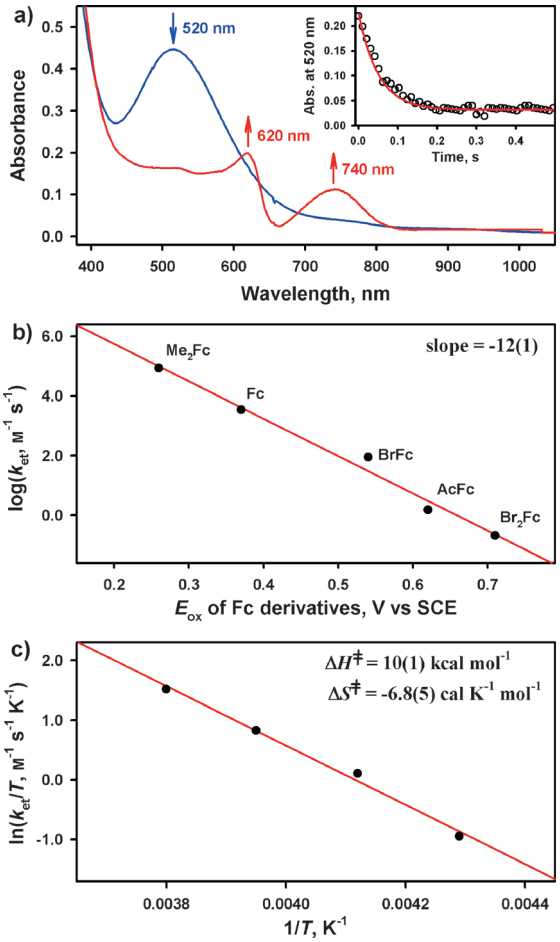

Figure 2. a) UV/Vis spectral changes showing the disappearance of the peak for $[(13\text{-TMC})Fe^{III}\text{-}OOC(CH_3)_3]^{2+}$ (**5**) at $\lambda = 520$ nm with the concomitant appearance of the peaks for $[(13\text{-TMC})Fe^{IV}(O)]^{2+}$ (**4**) at $\lambda = 740$ nm and Fc^+ at $\lambda = 620$ nm by addition of Fc (1.0 equiv) to a solution of **5** (0.50 mM, blue line) in acetone/CF_3CH_2OH (v/v 3:1) at −40 °C. Inset shows the time trace monitored at $\lambda = 520$ nm in the reaction of **5** (0.25 mM) and Fc (2.5 mM) in acetone/CF_3CH_2OH (v/v 3:1) at −40 °C. b) Plot of ln k_{et} against the E_{ox} of electron donors obtained in the electron-transfer reaction from Fc derivatives to **5** in acetone/CF_3CH_2OH (v/v 3:1) at −40 °C. c) The Eyring plot for electron transfer from bromoferrocene (BrFc) to **5** in acetone/CF_3CH_2OH (v/v 3:1) at 233–263 K.

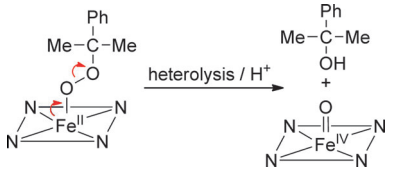

Scheme 2. Heterolytic O–O bond cleavage of nonheme iron(II) (hydro/alkyl)peroxo complexes.

 © 2014 Wiley-VCH Verlag GmbH & Co. KGaA, Weinheim

Given the fast O–O bond cleavage reactions, DFT calculations may provide a more detailed view on the reaction courses. It is known from earlier calculations that O–O bond-breaking reactions of Fe^{II}–OOH have a low energy barrier,[7c] and significantly more favorable than that of Fe^{III}–OOH.[7e] Figure 3 shows a comparison of O–O bond-breaking reactions in the three types of Fe^{n+}–OOH. For **2** specifically, the spontaneous homolytic O–O bond breaking was found to have a barrier of 26.3 kcal mol^{-1} (Figure 3, left).[4c] We calculate the corresponding reaction with **3** to have a barrier of 10.0 kcal mol^{-1} in a two-step reaction (Figure 3, center; see also Tables S3–S5), thus showing that the O–O bond breaking of Fe^{II}–OOH is indeed much easier than that of Fe^{III}–OOH. This data is in agreement with our experimental data, although one has to keep in mind that both of these calculated reactions are endothermic, and are thus not likely to occur spontaneously because of the lack of a driving force. Previous calculations on Fenton chemistry of this complex included explicit proton-donor models to address this issue.[8b] It was shown that the O–O bond breaking of the Fe^{II}–OOH species becomes, strictly speaking, a mixed homolytic and heterolytic character, but with a very-low-energy barrier (Figure 3, right, adapted from reference [8b]). This step is followed by a fast proton-coupled electron transfer (PCET), thus making it in total a heterolytic reaction.[8b]

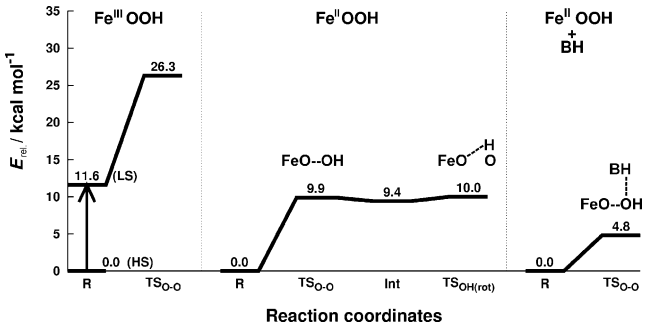

Figure 3. Comparison of three types of pathways for the O–O bond cleavage of Fe^{III}–OOH, Fe^{II}–OOH, and Fe^{II}–OOH + H^+. For Fe^{III}–OOH, a spin state change from high spin (HS, $S=5/2$) to low spin (LS, $S=1/2$) is seen to utilize the lowest lying transition state (TS; left).[4c] For Fe^{II}–OOH, the reaction occurs in two steps, where the first step forms a free •OH radical which rotates to form a hydrogen bond with $Fe^{III}O$ in the second step (center). If a proton is available, the barrier becomes even lower (right). The proton can be transferred without a barrier and coupled to an electron transfer from $Fe^{III}O$ (PCET).[8b]

In summary, we have shown very recently the conversion of an iron(III) peroxo complex binding redox-inactive metal ions into a high-valent iron(IV) oxo complex upon one-electron reduction.[11] In the present study, we have demonstrated that one-electron reduction of iron(III) (hydro/alkyl)peroxo complexes by Fc derivatives generates their corresponding iron(IV) oxo complexes. The electron transfer from electron donors to iron(III) (hydro/alkyl)peroxo complexes is the rate-determining step and the resulting iron(II) (hydro/alkyl)peroxo species are converted into iron(IV) oxo species rapidly by heterolytic O–O bond cleavage (Scheme 1 a, pathways B and C). To the best of our knowledge, the present results provide the first clear biomimetic example of nonheme iron enzymatic and Fenton reactions for the conversion of iron(II) (hydro/alkyl)peroxo into high-valent iron(IV) oxo species.

Received: April 22, 2014
Revised: May 13, 2014
Published online: June 10, 2014

Keywords: bioinorganic chemistry · enzyme models · iron · nonheme compounds · reaction mechanisms

[1] a) E. I. Solomon, T. C. Brunold, M. I. Davis, J. N. Kemsley, S.-K. Lee, N. Lehnert, F. Neese, A. J. Skulan, Y.-S. Yang, J. Zhou, *Chem. Rev.* **2000**, *100*, 235–349; b) M. Costas, M. P. Mehn, M. P. Jensen, L. Que, Jr., *Chem. Rev.* **2004**, *104*, 939–986; c) E. G. Kovaleva, J. D. Lipscomb, *Science* **2007**, *316*, 453–457; d) E. G. Kovaleva, J. D. Lipscomb, *Nat. Chem. Biol.* **2008**, *4*, 186–193; e) P. C. A. Bruijnincx, G. van Koten, R. J. M. K. Gebbink, *Chem. Soc. Rev.* **2008**, *37*, 2716–2744; f) E. I. Solomon, S. D. Wong, L. V. Liu, A. Decker, M. S. Chow, *Curr. Opin. Chem. Biol.* **2009**, *13*, 99–113; g) J. Cho, R. Sarangi, W. Nam, *Acc. Chem. Res.* **2012**, *45*, 1321–1330; h) E. I. Solomon, K. M. Light, L. V. Liu, M. Srnec, S. D. Wong, *Acc. Chem. Res.* **2013**, *46*, 2725–2739.

[2] J.-J. Girerd, F. Banse, A. J. Simaan, *Struct. Bonding (Berlin)* **2000**, *97*, 145–177.

[3] a) N. Lehnert, R. Y. N. Ho, L. Que, Jr., E. I. Solomon, *J. Am. Chem. Soc.* **2001**, *123*, 8271–8290; b) N. Lehnert, R. Y. N. Ho, L. Que, Jr., E. I. Solomon, *J. Am. Chem. Soc.* **2001**, *123*, 12802–12816; c) A. Wada, S. Ogo, S. Nagatomo, T. Kitagawa, Y. Watanabe, K. Jitsukawa, H. Masuda, *Inorg. Chem.* **2002**, *41*, 616–618; d) T. Kitagawa, A. Dey, P. Lugo-Mas, J. B. Benedict, W. Kaminsky, E. I. Solomon, J. A. Kovacs, *J. Am. Chem. Soc.* **2006**, *128*, 14448–14449; e) E. Nam, P. E. Alokolaro, R. D. Swartz, M. C. Gleaves, J. Pikul, J. A. Kovacs, *Inorg. Chem.* **2011**, *50*, 1592–1602; f) D. Krishnamurthy, G. D. Kasper, F. Namuswe, W. D. Kerber, A. A. N. Sarjeant, P. Moënne-Loccoz, D. P. Goldberg, *J. Am. Chem. Soc.* **2006**, *128*, 14222–14223; g) F. Namuswe, T. Hayashi, Y. Jiang, G. D. Kasper, A. A. N. Sarjeant, P. Moënne-Loccoz, D. P. Goldberg, *J. Am. Chem. Soc.* **2010**, *132*, 157–167; h) M. R. Bukowski, H. L. Halfen, T. A. van den Berg, J. A. Halfen, L. Que, Jr., *Angew. Chem.* **2005**, *117*, 590–593; *Angew. Chem. Int. Ed.* **2005**, *44*, 584–587; i) J. Bautz, P. Comba, L. Que, Jr., *Inorg. Chem.* **2006**, *45*, 7077–7082; j) M. P. Jensen, A. M. i Payeras, A. T. Fiedler, M. Costas, J. Kaizer, A. Stubna, E. Münck, L. Que, Jr., *Inorg. Chem.* **2007**, *46*, 2398–2408; k) M. S. Seo, T. Kamachi, T. Kouno, K. Murata, M. J. Park, K. Yoshizawa, W. Nam, *Angew. Chem.* **2007**, *119*, 2341–2344; *Angew. Chem. Int. Ed.* **2007**, *46*, 2291–2294.

[4] a) J. Cho, S. Jeon, S. A. Wilson, L. V. Liu, E. A. Kang, J. J. Braymer, M. H. Lim, B. Hedman, K. O. Hodgson, J. S. Valentine, E. I. Solomon, W. Nam, *Nature* **2011**, *478*, 502–505; b) F. Li, K. K. Meier, M. A. Cranswick, M. Chakrabarti, K. M. Van Heuvelen, E. Münck, L. Que, Jr., *J. Am. Chem. Soc.* **2011**, *133*, 7256–7259; c) L. V. Liu, S. Hong, J. Cho, W. Nam, E. I. Solomon, *J. Am. Chem. Soc.* **2013**, *135*, 3286–3299; d) S. Hong, Y.-M. Lee, K.-B. Cho, M. S. Seo, D. Song, J. Yoon, R. Garcia-Serres, M. Clémancey, T. Ogura, W. Shin, J.-M. Latour, W. Nam, *Chem. Sci.* **2014**, *5*, 156–162.

[5] a) J. E. Baldwin, M. Bradley, *Chem. Rev.* **1990**, *90*, 1079–1088; b) W. A. van der Donk, C. Krebs, J. M. Bollinger, Jr., *Curr. Opin. Struct. Biol.* **2010**, *20*, 673–683; c) J. M. Ogle, I. J. Clifton, P. J. Rutledge, J. M. Elkins, N. I. Burzlaff, R. M. Adlington, P. L. Roach, J. E. Baldwin, *Chem. Biol.* **2001**, *8*, 1231–1237.

 © 2014 Wiley-VCH Verlag GmbH & Co. KGaA, Weinheim

[6] a) M. M. Abu-Omar, A. Loaiza, N. Hontzeas, *Chem. Rev.* **2005**, *105*, 2227 – 2252; b) A. Bassan, T. Borowski, P. E. M. Siegbahn, *Dalton Trans.* **2004**, 3153 – 3162; c) M. S. Chow, B. E. Eser, S. A. Wilson, K. O. Hodgson, B. Hedman, P. F. Fitzpatrick, E. I. Solomon, *J. Am. Chem. Soc.* **2009**, *131*, 7685 – 7698.

[7] a) H. J. H. Fenton, *J. Chem. Soc. Trans.* **1894**, *65*, 899 – 910; b) S. Enami, Y. Sakamoto, A. J. Colussi, *Proc. Natl. Acad. Sci. USA* **2014**, *111*, 623 – 628; c) F. Buda, B. Ensing, M. C. M. Gribnau, E. J. Baerends, *Chem. Eur. J.* **2001**, *7*, 2775 – 2783; d) G. Gopakumar, P. Belanzoni, E. J. Baerends, *Inorg. Chem.* **2012**, *51*, 63 – 75; e) B. Ensing, F. Buda, E. J. Baerends, *J. Phys. Chem. A* **2003**, *107*, 5722 – 5731.

[8] a) F. Li, J. England, L. Que, Jr., *J. Am. Chem. Soc.* **2010**, *132*, 2134 – 2135; b) H. Hirao, F. Li, L. Que, Jr., K. Morokuma, *Inorg. Chem.* **2011**, *50*, 6637 – 6648.

[9] S. Fukuzumi, Y. Morimoto, H. Kotani, P. Naumov, Y.-M. Lee, W. Nam, *Nat. Chem.* **2010**, *2*, 756 – 759.

[10] Y.-M. Lee, H. Kotani, T. Tomoyoshi, W. Nam, S. Fukuzumi, *J. Am. Chem. Soc.* **2008**, *130*, 434 – 435.

[11] a) Y.-M. Lee, S. Bang, Y. M. Kim, J. Cho, S. Hong, T. Nomura, T. Ogura, O. Troeppner, I. Ivanovíc-Burmazovíc, R. Sarangi, S. Fukuzumi, W. Nam, *Chem. Sci.* **2013**, *4*, 3917 – 3923; b) F. Li, K. M. Van Heuvelen, K. K. Meier, E. Münck, L. Que, Jr., *J. Am. Chem. Soc.* **2013**, *135*, 10198 – 10201.

[12] S. Hong, H. So, H. Yoon, K.-B. Cho, Y.-M. Lee, S. Fukuzumi, W. Nam, *Dalton Trans.* **2013**, *42*, 7842 – 7845.

[13] a) D. Das, Y.-M. Lee, K. Ohkubo, W. Nam, K. D. Karlin, S. Fukuzumi, *J. Am. Chem. Soc.* **2013**, *135*, 2825 – 2834; b) L. Tahsini, H. Kotani, Y.-M. Lee, J. Cho, W. Nam, K. D. Karlin, S. Fukuzumi, *Chem. Eur. J.* **2012**, *18*, 1084 – 1093; c) T. F. Markle, I. J. Rhile, J. M. Mayer, *J. Am. Chem. Soc.* **2011**, *133*, 17341 – 17352.

[14] a) D. V. Avila, C. E. Brown, K. U. Ingold, J. Lusztyk, *J. Am. Chem. Soc.* **1993**, *115*, 466 – 470; b) M. Costas, K. Chen, L. Que, Jr., *Coord. Chem. Rev.* **2000**, *200 – 202*, 517 – 544; c) T. Tano, H. Sugimoto, N. Fujieda, S. Itoh, *Eur. J. Inorg. Chem.* **2012**, 4099 – 4103; d) M. K. Coggins, V. Martin-Diaconescu, S. DeBeer, J. A. Kovacs, *J. Am. Chem. Soc.* **2013**, *135*, 4260 – 4272.

 © 2014 Wiley-VCH Verlag GmbH & Co. KGaA, Weinheim